Progress In Electromagnetics Research C, Vol. 41, 239–254, 2013

A COMPACT WIDEBAND BANDPASS FILTER USING NOVEL CSRR LOADED QMSIW RESONATOR WITH HIGH SELECTIVITY

Hailin Cao[1, 2, *], Sijia He[1], Hao Li[1], and Shizhong Yang[1, 2]

[1]The Center of Communication and Tracking Telemetering & Command, Chongqing University, Chongqing 400044, People's Republic of China

[2]Key Laboratory of Aerocraft Tracking, Telemetering & Command and Communication, Ministry of Education, Chongqing University, Chongqing 400044, People's Republic of China

Abstract—A novel quarter-mode substrate integrated waveguide (QMSIW) resonator with back-to-back triangular complementary split-ring resonators (CSRRs) etched on the waveguide surface is proposed in this paper. The proposed CSRR structures allow the implementation of a forward-wave passband propagating with high selectivity below the characteristic cutoff frequency of the conventional QMSIW. Utilizing the property of flexible open structure on QMSIWs' two sides, a cascaded quadruplet (CQ) bandpass filter (BPF) using the proposed QMSIW resonator and proximity coupling structure is presented. Compared with some other reported BPFs with SIW technique, the presented BPF using the novel QMSIW resonator has great improvements on size reduction and selectivity, simultaneously, with simple geometry. At the center frequency of 3.7 GHz, the designed BPF filter achieves a wideband with a fractional bandwidth up to 24.3% and a high selectivity with a shape factor of 1.23. The compact dimension of this filter is as small as $0.36\lambda_g \times 0.36\lambda_g$, where λ_g is the guide wavelength at the center frequency. The proposed filter is simulated, fabricated and tested. The measured results are in good agreement with the simulation.

Received 30 May 2013, Accepted 6 July 2013, Scheduled 11 July 2013

* Corresponding author: Hailin Cao (hailincao@cqu.edu.cn).

1. INTRODUCTION

The emerging substrate integrated waveguide (SIW) technique has been proven to be effective in the integration of planar and nonplanar circuits by using easy and low-cost standard PCB or LTCC fabrication process [1,2]. Then, the traditional non-planar hollow rectangular waveguide can effectively be synthesized into planar substrate with metalized slots or trenches or even arrays of metallic via posts. Compared with other planar components using microstrip or co-planar waveguide (CPW) schemes, SIW components have shown excellent performances such as high Q-factor and low insertion loss [3–8], however, which always have much larger size than their microstrip or CPW counterparts.

Because the field distribution in the SIW cavity is symmetrical, recently, the concept 'half mode substrate integrated waveguide (HMSIW)' [9–12] and 'quarter-mode substrate integrated waveguide (QMSIW)' [13,14] have attracted much interest in the design of bandpass filter. Compared with SIW, HMSIW has nearly 50% reduction and QMSIW has nearly 75% reduction in size, respectively. The Q value of QMSIW structure is usually lower than their conventional SIW and HMSIW counterparts since the two open edges are not perfect magnetic walls and some amount of radiation may happen [13]. However, the QMSIW can obtain a much stronger coupling coefficient between two neighbor sections with proper coupling means. In [15], the QMSIW cavity and a novel negative coupling structure have been used to enhance the selectivity of cross-coupled BPF with a quasi-elliptic response.

It has been demonstrated that complementary split ring resonators (CSRRs) etched on the ground plane or on the conductor strip of planar transmission media (microstrip or CPW) provide a negative effective permittivity to the structure, and signal propagation is precluded (stopband behavior) in the vicinity of their resonant frequency [16]. This property has been applied to the design of bandstop, bandpass, and ultra-wide bandpass filters for high performance. The CSRRs etched on the top plane of the SIW for transmission zero control was first proposed by Zhang et al. in [17] and then re-clarified in [18]. It was further extensively studied by Dong et al. in [19]. CSRR is also used to the design of HMSIW bandpass filter [20] with sharp rejection skirt and SIW diplexer [21]. In [22], the coupling effect between CSRR and SIW cavity is used to reduce the resonance frequency of a conventional SIW cavity.

With the rapid growth of the miniaturized portable communication terminal, compact BPF with high performance has been great in demand. When high selectivity and/or other requirements cannot be met by the filters with a single pair of transmission zeros, cross-coupling topologies are widely used to introduce additional transmission zeros for BPF applications [23–26]. The cascaded quadruplet (CQ) filter consists of cascaded sections of four resonators, each with one cross coupling. The cross coupling can be arranged in such a way that a pair of attenuation poles are introduced at the finite frequencies to improve the selectivity [27]. As compared with other types of filters that involve more than one pair of transmission zeros, the significant advantage of CQ filters lies in their simpler tunability, because the effect of each cross coupling is independent.

In this paper, a novel QMSIW resonator with back-to-back triangular CSRRs etched on the waveguide surface is proposed. Based on the coupling matrix synthesis method for microwave filters, utilizing the characteristic of flexible open structure on QMSIWs' two sides, a CQ BPF using the proposed QMSIW resonator and proximity coupling structure is presented.

2. TRIANGULAR CSRR-QMSIW RESONATOR

2.1. Structures

The geometric structure of the proposed QMSIW resonator is shown in Figure 1. Two crossed linear arrays of metallized vias are used to form the electric sidewalls of the waveguide. A pair of back-to-back triangle CSRRs are adopted and etched on the metal cover of the

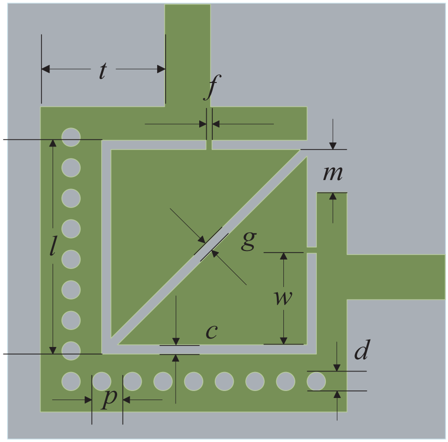

Figure 1. Triangular CSRR-QMSIW cell.

waveguide. The ground remains as a solid ground in the design, which is not depicted in Figure 1. The 50 Ω microstrip feed-line used here is for the purpose of measurement. The substrate of Taconic TLT with a thickness of 1 mm and a relative permittivity of 2.55 is used in all of our designs. And the simulation is done on the full-wave EM-Simulator (HFSS). The metalized vias have a diameter of 0.6 mm and a center to center spacing of 1 mm. The surface current of the triangle CSRR loaded QMSIW has to detour around the CSRR, which stretches the effective current path. Figure 2 shows the surface current distribution of a QMSIW (a) and the proposed CSRR loaded QMSIW (b).

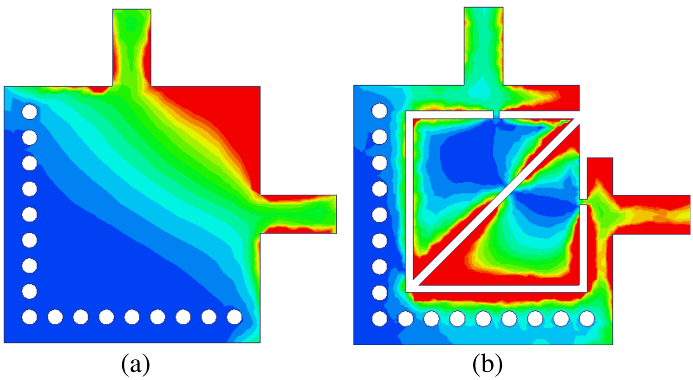

Figure 2. Surface current distribution. (a) Conventional QMSIW, (b) the proposed CSRR loaded QMSIW.

2.2. Parameters Analyze

A parametric study of the proposed resonator about f, g, w and t is shown in Figures 3–6, respectively. The initial values of the triangular CSRR-QMSIW cell are as follows: $c = 0.3$ mm, $d = 0.6$ mm, $m = 1.5$ mm, $p = 1$ mm, $l = 7$ mm. As depicted in Figure 3, when $g = 0.3$ mm, $w = 3.1$ mm, $t = 4.05$ mm is fixed and the split width f increases from 0.2 to 1 mm, the resonant frequency changes from 4 to 4.3 GHz. Figure 4 shows the effect of the slot width g on resonator. When $f = 0.2$ mm, $w = 3.1$ mm and $t = 4.05$ mm is fixed, the shorter the slot length is, the lower the resonator frequency is. As shown in Figure 5, when $f = 0.2$ mm, $g = 0.3$ mm, $t = 4.05$ mm is fixed and the split position w changes from 2.5 to 4.5 mm, the resonant frequency changes from a high frequency to a low one, but at the same time, the insert loss will increase. Thus w is decided to be 3.1 mm finally for reasonable compromise. In Figure 6, when $g = 0.3$ mm, $w = 3.1$ mm and $f = 0.2$ mm is fixed and feed-line offset t is small, the feeding

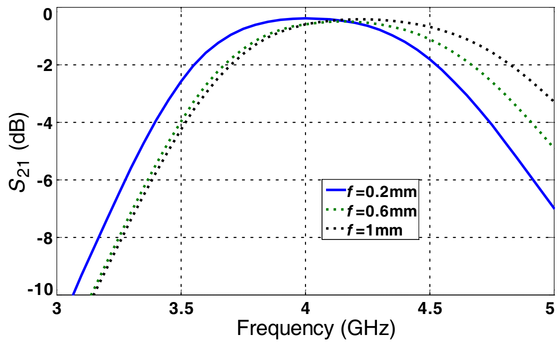

Figure 3. Simulated S_{21} of CSRR-QMSIW resonator with $f = 0.2\,\text{mm}$, $f = 0.6\,\text{mm}$, $f = 1\,\text{mm}$.

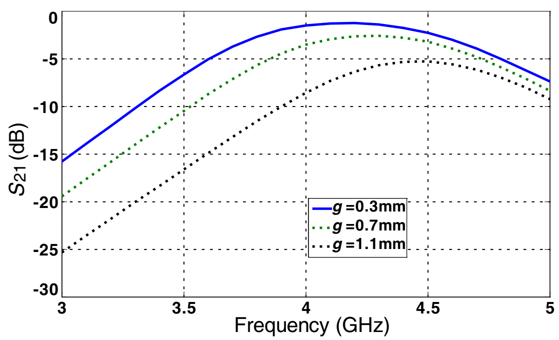

Figure 4. Simulated S_{21} of CSRR-QMSIW resonator with $g = 0.3\,\text{mm}$, $g = 0.7\,\text{mm}$, $g = 1.1\,\text{mm}$.

is closed to the edge of the CSRR-QMSIW and the current can not effectively propagate because of the metallized vias. As t gets bigger, the resonant frequencies become higher and the insert loss increases. By properly adjusting the parameters of the slots, a lower resonant frequency is achieved without altering the overall size of the resonator.

With this carefully designed CSRR, the resonant frequency of the proposed CSRR-QMSIW is significantly reduced as we can see in Figure 7. The conventional QMSIW resonator has a resonant frequency at 8.2 GHz, and the proposed CSRR-QMSIW has a resonant frequency at 4 GHz. Although there is a third harmonic frequency at about 11.4 GHz for CSRR-QMSIW resonator, it can be easily restrained by the stacking effect of the upcoming cascaded structure. The proposed CSRR structure allows the implementation of a forward-wave

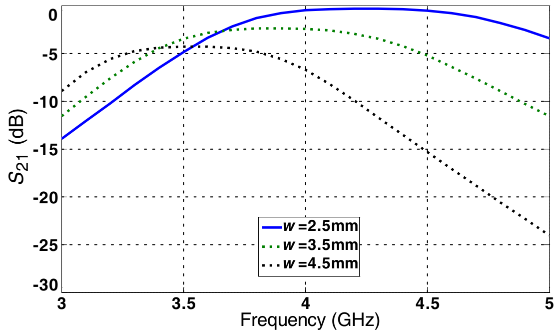

Figure 5. Simulated S_{21} of CSRR-QMSIW resonator with $w = 2.5\,\mathrm{mm}$, $w = 3.5\,\mathrm{mm}$, $w = 4.5\,\mathrm{mm}$.

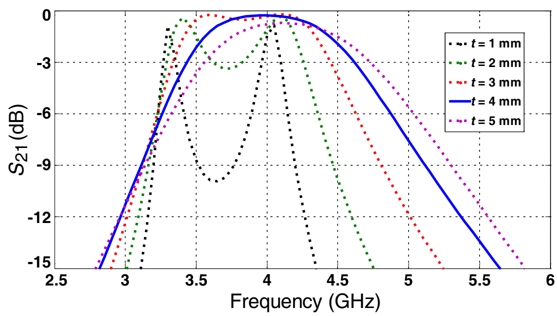

Figure 6. Simulated S_{21} of CSRR-QMSIW resonator with $t = 1\,\mathrm{mm}$, $t = 2\,\mathrm{mm}$, $t = 3\,\mathrm{mm}$, $t = 4\,\mathrm{mm}$, $t = 5\,\mathrm{mm}$.

passband propagating with high selectivity below the characteristic cutoff frequency of the conventional QMSIW. This novel structure provides an excellent strategy for designing compact low frequency filter.

The lumped-element equivalent-circuit model (see Figure 8) has been derived to demonstrate the transmission characteristics. Material losses are neglected in the model. As seen in Figure 8, the QMSIW can be considered as an ordinary two-wire transmission line (formed by the metal surface and the ground) loaded with infinite number of short-circuited stubs (formed by via-walls). Viewed from the center of the waveguide, the short-circuited stub (via-walls) appears as inductive after a piece of transmission line and it is modeled as L_d. The CSRR is modeled by means of the shunt-connected resonant tank formed by the capacitance C_r and the inductance L_r. Due to the non-zero m

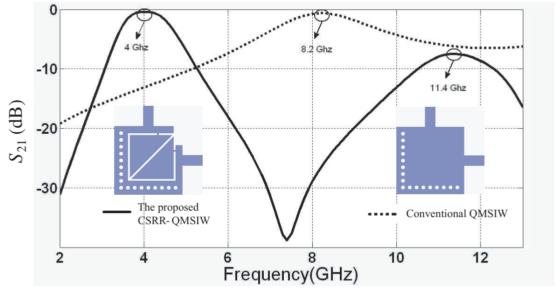

Figure 7. Full-wave simulated S_{21} of conventional QMSIW and the proposed CSRR-QMSIW.

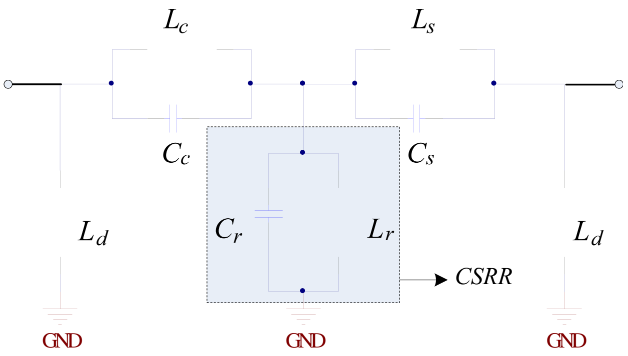

Figure 8. Equivalent lumped circuit of the proposed CSRR-QMSIW resonator.

for wideband performance and the slightly asymmetrical configuration between the two open sides, the inductive connection between the waveguide transmission line and the back-to-back triangle CSRRs is represented by L_c, L_s, respectively; The capacitive coupling, which is realized by the slot coupling between the waveguide transmission line and CSRRs, is denoted by C_c, C_s, respectively.

To demonstrate the validity of the equivalent lumped circuit model, the comparison between the CSRR-QMSIW resonant cell simulated by HFSS and the equivalent circuit model simulated by Advanced Design System (ADS) is shown in Figure 9. As can be seen, the equivalent circuit model simulation agrees well with the full-wave HFSS simulation, with the equivalent network parameters $L_r = 0.42\,\text{nH}$, $C_r = 3.8\,\text{pF}$, $L_c = 8.37\,\text{nH}$, $C_c = 1.0\,\text{pF}$, $L_s = 1.0\,\text{nH}$, $C_s = 0.48\,\text{pF}$, $L_d = 10\,\text{nH}$.

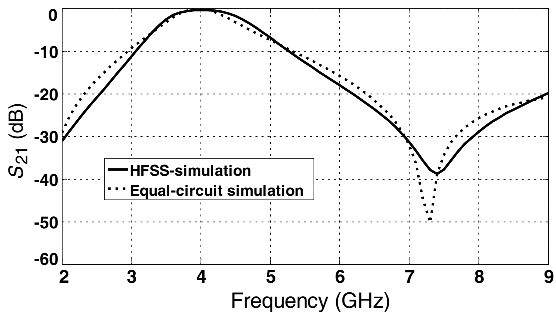

Figure 9. Transmission responses by equivalent circuit model and full-wave simulation.

3. FILTER ANALYSIS AND DESIGN

3.1. The Configuration of the Proposed Filter

Figure 10 illustrates geometry and coupling structures of the proposed CQ filter, where each node represents a resonator, the full lines indicate the direct couplings, and the broken line denotes the proximity couplings. The filter design methodology starts from the design parameters, including the coupling coefficient and external quality factor, which can be determined in terms of the circuit elements of a low-pass prototype filter [27]. Based on the proposed design strategy, this section designs a fourth-order BPF with a center frequency of 3.7 GHz, fractional bandwidth of 24%, return loss of −20 dB, and two transmission zeros allocated at 3 GHz and 4.4 GHz (transmission zeros at $\pm j1.43$), respectively. The design parameters associated with the specifications may be expressed as [27]:

$$\omega_{a1} = \omega_0 \frac{-\Omega_a \mathrm{FBW} + \sqrt{(\Omega_a \mathrm{FBW})^2 + 4}}{2} \tag{1}$$

$$\omega_{a2} = \omega_0 \frac{\Omega_a \mathrm{FBW} + \sqrt{(\Omega_a \mathrm{FBW})^2 + 4}}{2} \tag{2}$$

$$M_{i,i+1} = M_{n-1,n-i+1} = \frac{\mathrm{FBW}}{\sqrt{g_i g_{i+1}}}, \quad \text{for} \quad i = 1 \text{ to } m-1 \tag{3}$$

$$M_{m,m+1} = \frac{\mathrm{FBW} \cdot J_m}{g_m} \tag{4}$$

FBW is the fractional bandwidth, g_i the lowpass prototype parameter, and ω_{a1} and ω_{a2} are the locations of two finite frequency attenuation poles of the bandpass filter. $\pm\Omega_a$ are the transmission zeros of the normalized complex plane. The corresponding coupling matrix [M] and the required external quality factor Q_e of this filter are given as follows [27]:

$$M = \begin{bmatrix} 0 & 0.19 & 0 & 0 \\ 0.19 & 0 & 0.53 & 0 \\ 0 & 0.53 & 0 & 0.19 \\ 0 & 0 & 0.19 & 0 \end{bmatrix} \tag{5}$$

$$Q_{ei} = Q_{eo} = 4.01 \tag{6}$$

It is a CQ filter with four CSRR loaded QMSIWs. The center frequency of the filter is determined by the resonant frequency of the constitutional resonators, while the bandwidth is mainly affected by the coupling strength.

3.2. Proximity Coupling

Figure 10 shows the designed coupling topology of the proposed cascaded bandpass filter. Two 50 Ω microstrip lines are employed as the I/O feed-lines. M_{ij} is the coupling coefficient between the resonators i and j, and Q_{ei} and Q_{eo} are the external quality factors in association with the input and output couplings, respectively. To determine the internal coupling coefficient, the pair of cascaded resonators is required to be excited with a high external Q factor in order to clearly

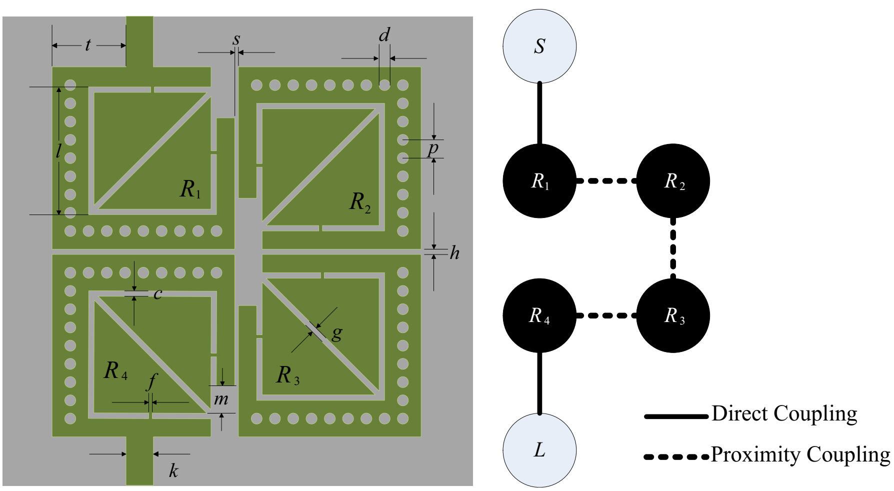

Figure 10. The proposed CQ filter and its general coupling structure.

observe the two resonance frequencies. Here we choose the eigenmode simulation to obtain the resonance frequencies.

Two types of coupling structures are shown in Figures 11 and 12, respectively. For the coupling configuration shown in Figure 11, two eigen modes around 3.7 GHz, also known as even and odd modes, are observed. The coupling coefficient, which is calculated by the formula [17–19]:

$$M = \frac{f_1^2 - f_2^2}{f_1^2 + f_2^2} \tag{7}$$

where f_1 and f_2 denote the resonance frequencies of the low and high modes respectively and can be adjusted by changing the distance s. Likewise, the vector electric field distribution, the resonance frequencies and the another coupling coefficient versus the distance h between resonators are shown in Figure 12.

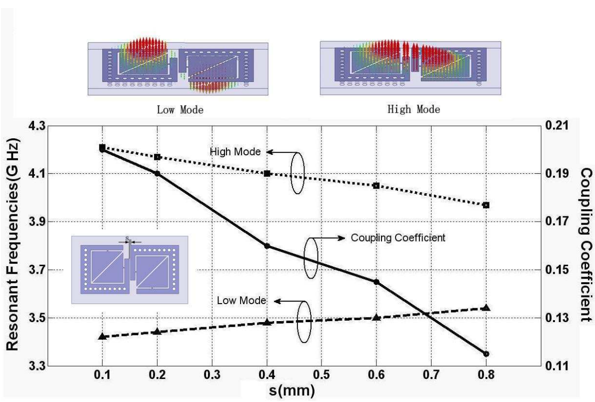

Figure 11. Vector electric field distribution, resonance frequencies of the two excited modes and the calculated coupling coefficient versus the distance s.

Since the resonant frequency of the odd mode is lower than that of the even mode, the coupling is electric in nature. Aperture coupled SIW resonators implement magnetic coupling easily, but have difficulty implementing electric coupling [27]. Here, with the proposed proximity coupling structure, electric coupling is readily realized, which facilitates the design of cascaded SIW filters. A 50 Ω feed-line was directly tapped onto the input/output QMSIW cavities. Because of the open structure on QMSIWs' two sides, the radiation may happen and the feeding position has a significant impact on the external quality factor Q_e.

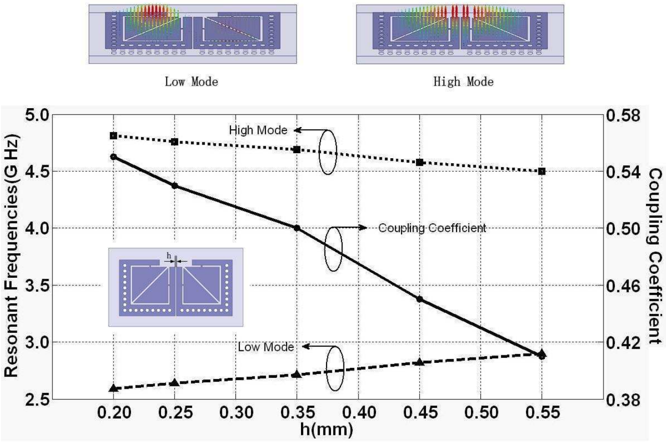

Figure 12. Vector electric field distribution, resonance frequencies of the two excited modes and the calculated coupling coefficient versus the distance h.

From the discussion of Figure 6 in **Parameters Analyze**, a proper external quality factor Q_e is achieved by adjusting the taper position t.

3.3. Filter Parameters

The design parameters above are used to estimate the initial sizes of the entire filter. Through the use of design curves, as shown in Figures 11–12, a fine-tuning procedure is used to optimize the entire filter. Table 1 gives dimensions after optimization.

Table 1. Dimensions of the proposed CQ bandpass filter.

Symbol	Value (mm)	Symbol	Value (mm)
t	4.05	c	0.3
s	0.2	g	0.3
h	0.25	f	0.2
d	0.6	m	1.5
p	1	l	7
w	3.1	k	1.5

4. MEASURED RESULTS AND DISCUSSION

To demonstrate the validity of the design strategies, one prototype of the proposed filter is fabricated by a double layer printed circuit board (PCB) process on a 1 mm thick Taconic TLT substrate with the permittivity of 2.55 and loss tangent of 0.0006. The size of the filter is 20.2×20.2 mm excluding the feed-line. A photograph of the filter is shown in Figure 13.

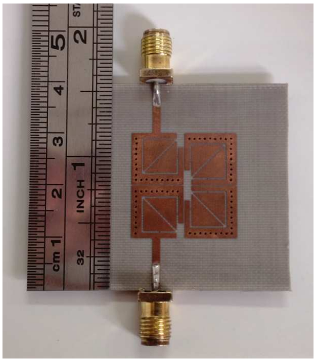

Figure 13. Photograph of fabricated BPF.

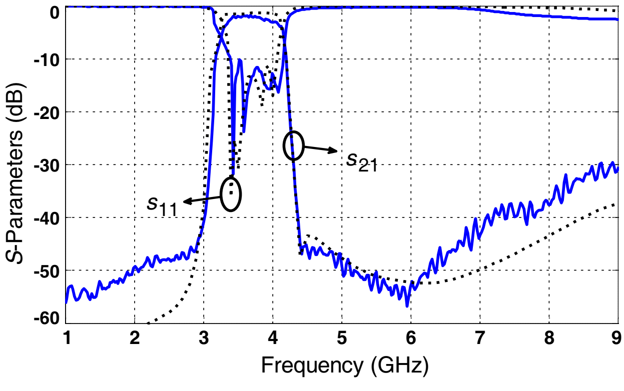

Figure 14. Measured and simulated results of the proposed BPF.

Figure 14 shows the measured results from 1 to 9 GHz compared with the simulated results by HFSS. The measured insertion loss is approximately 1.8 dB at 3.7 GHz and the return loss is better than 10 dB from 3.4 to 4.2 GHz. The 3 dB bandwidth is 0.9 GHz and

Table 2. Comparison with the referenced filters.

Ref.	f_0 (GHz)	Size (λ_g^2)	FBW	Shape Factor (20/3 dB)	Applied Structures
[11]	5.8	0.80	14%	1.5	HMSIW
[13]-1	5.85	0.31	14%	2.03	QMSIW
[13]-2	5.5	0.29	26%	2.16	QMSIW
[14]-1	20.5	2.49	3.41%	2.0	QMSIW
[14]-2	20.5	1.68	3.90%	1.5	QMSIW
[15]	5.57	0.25	7.44%	2.38	QMSIW
[17]	8.15	0.55	23%	1.79	SIW,CSRR
[20]	3.52	0.176	6.25%	1.36	SIW,CSRR
[22]-1	5.03	0.71	6.36%	2.97	SIW,CSRR
[22]-2	5.03	0.88	6.36%	1.56	SIW,CSRR
Proposed	3.7	0.13	24.3%	1.23	QMSIW,CSRR

Notes: FBW $= \frac{f_{3\,\mathrm{dB}}}{f_0}$, Shape Factor (20/3 dB) $= \frac{\mathrm{BW}_{20\,\mathrm{dB}}}{\mathrm{BW}_{3\,\mathrm{dB}}}$.

the 20 dB bandwidth is 1.11 GHz. The filter has a shape factor of 1.11/0.9 = 1.23. The filter has a fractional bandwidth of 24.3%. The transmission zero point, at approximately 4.4 GHz, considerably improves the selectivity of the upper stop band. The increased insert loss may be resulted by the limited fabrication accuracy of vias, shrinking the effective size of the cavity.

Table 2 shows the performance comparison of the proposed filter with the other reported SIW BPFs. Compared with the recently reported BPFs using SIW technique in [11, 13–15, 17, 20, 22], the proposed filter has a more compact size, much wider FBW and much sharper frequency selectivity. Type 2 in [13] has a FBW up to 26%, but its frequency selectivity is poor.

5. CONCLUSION

A novel QMSIW resonator with back-to-back triangular CSRRs etched on the waveguide surface is proposed in this paper. Compared with conventional QMSIW resonator, the proposed CSRR loaded QMSIW resonator achieves a 51% reduction in size. Utilizing the characteristic of flexible open structure on QMSIWs' two sides, a CQ BPF using the proposed QMSIW resonator and proximity coupling structure is presented. Compared with some previously reported BPFs using SIW technique, the presented BPF using the novel QMSIW resonator has great improvements on size reduction and selectivity, simultaneously, with simple geometry. At the center frequency of 3.7 GHz, the designed BPF filter achieves a wideband with a fractional bandwidth up to 24.3% and a high selectivity with a shape factor of 1.23 at 20/3 dB. The compact dimension of this filter is as small as $0.36\lambda_g \times 0.36\lambda_g$, where λ_g is the guide wavelength at the center frequency.

ACKNOWLEDGMENT

This work is supported by the Fundamental Research Funds for the Central Universities of CQU (CDJPY12160001), also partly by the National Natural Science Foundation of China under Contract No. 60501023 and the Natural Science Foundation Project of CQ CSTC (CSTC 2010BB2243, CSTC 2013JJB40005).

REFERENCES

1. Cassivi, Y., L. Perregrini, P. Arcioni, M. Bressan, K. Wu, and G. Conciauro, "Dispersion characteristics of substrate integrated rectangular waveguide," *IEEE Microw. Wirel. Compon. Lett.*, Vol. 12, No. 9, 333–335, Sep. 2002.
2. Deslandes, D. and K. Wu, "Accurate modeling, wave mechanism, and design consideration of a substrate integrated waveguide," *IEEE Trans. on Microw. Theory and Tech.*, Vol. 54, No. 6, 2516–2526, Jun. 2006.
3. Djerafi, T., N. J. G. Fonseca, and K. Wu, "Design and implementation of a planar 4 × 4 Butler matrix in SIW technology for wide band high power applications," *Progress In Electromagnetics Research B*, Vol. 35, 29–51, 2011.
4. Cheng, Y. J., "Substrate integrated waveguide frequency-agile slot antenna and its multibeam application," *Progress In Electromagnetics Research*, Vol. 130, 153–168, 2012.
5. Su, P., Z. X. Tang, and B. Zhang, "Push-push dielectric resonator oscillator using substrate integrated waveguide power combiner," *Progress In Electromagnetics Research Letters*, Vol. 30, 105–113, 2012.
6. Wang, R., L. S. Wu, and X. L. Zhou, "Compact folded substrate integrated waveguide cavities and bandpass filter," *Progress In Electromagnetics Research*, Vol. 84, 135–147, 2008.

7. Ismail, A., M. S. Razalli, M. A. Mahdi, R. S. A. R. Abdullah, N. K. Noordin, and M. F. A. Rasid, "X-band trisection substrate-integrated waveguide quasi-elliptic filter," *Progress In Electromagnetics Research*, Vol. 85, 133–145, 2008.
8. Huang, Y. M., Z. H. Shao, and L. F. Liu, "A substrate integrated waveguide bandpass filter using novel defected ground structure shape," *Progress In Electromagnetics Research*, Vol. 135, 201–213, 2013.
9. Wang, Y. Q., W. Hong, Y. D. Dong, B. Liu, H. J. Tang, J. X. Chen, X. X. Yin, and K. Wu, "Half mode substrateintegrated waveguide (HMSIW) bandpass filter," *IEEE Microw. Wirel. Compon. Lett.*, Vol. 17, No. 4, 265–267, Apr. 2007.
10. Song, Q. Y., H. R. Cheng, X. H. Wang, L. Xu, X. Q. Chen, and X. W. Shi, "Novel wideband bandpass filter integrating HMSIW and DGS," *Journal of Electromagnetic Waves and Applications*, Vol. 23, Nos. 14–15, 2031–2040, 2009.
11. Gong, K., W. Hong, H. J. Tang, and J. X. Chen, "C-band bandpass filter based on half mode substrate integrated waveguide (HMSIW) cavities," *2009 Asia-Pacific Microwave Conference,* Singapore, Dec. 2009.
12. Wang, Z., X. Li, S. Zhou, B. Yan, R.-M. Xu, and W. Lin, "Half mode substrate integrated folded waveguide (HMSIFW) and partial H-plane bandpass filter," *Progress In Electromagnetics Research*, Vol. 101, 203–216, 2010.
13. Zhang, Z., N. Yang, and K. Wu, "5 GHz bandpass filter demonstration using quarter-mode substrate integrated waveguide cavity for wireless system," *2009 Radio and Wireless Symposium*, San Diego, Jan. 2009.
14. Chen, X. P. and K. Wu, "Substrate integrated waveguide cross-coupled filter with negative coupling structure," *IEEE Trans. Microw. Theory Tech.*, Vol. 56, No. 1, 2008.
15. Guo, Z., K. S. Chin, W. Che, and C. C. Chang, "Cross-coupled bandpass filters using QMSIW cavities and S-shaped slot coupling structures," *Journal of Electromagnetic Waves and Applications*, Vol. 27, No. 2, 160–167, 2013.
16. Falcone, F., T. Lopetegi, J. D. Baena, R. Marqudes, F. Martin, and M. Sorolla, "Effective negative-ε stop-band microstrip lines based on complementary split ring resonators," *IEEE Microw. Wireless Compon. Lett.*, Vol. 14, No. 6, 280–282, Jun. 2004.
17. Zhang, X., Z. Yu, and J. Xu, "Novel band-pass substrate integrated waveguide (SIW) filter based on complementary split ring resonators (CSRRs)," *Progress In Electromagnetics Research*,

Vol. 72, 39–46, 2007.

18. Wu, L. S., X. L. Zhou, Q. F. Wei, and W. Y. Yin, "An extended doublet substrate integrated waveguide (SIW) bandpass filter with a complementary split ring resonator (CSRR)," *IEEE Microw. Wirel. Compon. Lett.*, Vol. 19, No. 12, Dec. 2009.
19. Dong, Y. D., T. Yang, and T. Itoh, "Substrate integrated waveguide loaded by complementary split-ring resonators and its applications to miniaturized waveguide filters," *IEEE Trans. Microw. Theory Tech.*, Vol. 57, No. 9, 2211–2223, Sept. 2009.
20. Zhang, Q. L., W. Y. Yin, S. L. He, and L. S. Wu, "Compact substrate integrated waveguide (SIW) bandpass filter with complementary split-ring resonators (CSRRs)," *IEEE Microw. Wirel. Compon. Lett.*, Vol. 20, No. 8, Aug. 2010.
21. Dong, Y. D. and T. Itoh, "Substrate integrated waveguide loaded by complementary split-ring resonators for miniaturized diplexer design," *IEEE Microw. Wirel. Compon. Lett.*, Vol. 21, No. 1, Jan. 2011.
22. Jiang, W., W. Shen, L. Zhou, and W. Y. Yin, "Miniaturized and high-selectivity substrate integrated waveguide (SIW) bandpass filter loaded by complementary split-ring resonators (CSRRs)," *Journal of Electromagnetic Waves and Applications*, Vol. 26, Nos. 11–12, 1448–1459, Aug. 2012.
23. Xu, Z. Q., Y. Shi, C. Y. Xu, and P. Wang, "A novel dual mode substrate integrated waveguide filter with mixed source-load coupling (MSLC)," *Progress In Electromagnetics Research*, Vol. 136, 595–606, 2013.
24. Chu, Q. X. and H. Wang, "A compact open-loop filter with mixed electric and magnetic coupling," *IEEE Trans. Microw. Theory Tech.*, Vol. 56, No. 2, Feb. 2008.
25. Lee, K., T. H. Lee, Y. S. Kim, and J. Lee, "New negative coupling structure for substrate-integrated cavity resonators and its application to design of an elliptic response filter," *Progress In Electromagnetics Research*, Vol. 137, 117–127, 2013.
26. Jedrzejewski, A., N. Leszczynska, L. Szydlowski, and M. Mrozowski, "Zero-pole approach to computer aided design of in-line siw filters with transmission zeros," *Progress In Electromagnetics Research*, Vol. 131, 517–533, 2012.
27. Hong, J. S. and M. Lancaster, *Microstrip Filters for RF/Microwave Applications*, John Wiley & Sons, Inc., 2001.